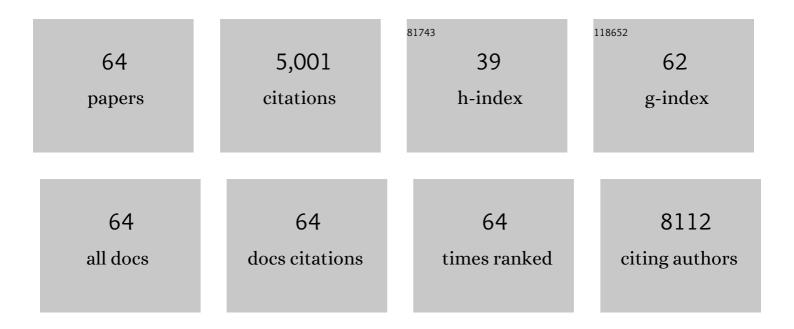
Ping Wang

List of Publications by Year in descending order

Source: https://exaly.com/author-pdf/5836572/publications.pdf Version: 2024-02-01



| # | Article | IF | CITATIONS |
|----|--|-----|-----------|
| 1 | Enzyme-like Fe-N5 single atom catalyst for simultaneous electrochemical detection of dopamine and uric acid. Journal of Electroanalytical Chemistry, 2022, 904, 115956. | 1.9 | 17 |
| 2 | High-Entropy Oxide for Highly Efficient Luminol–Dissolved Oxygen Electrochemiluminescence and Biosensing Applications. Analytical Chemistry, 2022, 94, 2958-2965. | 3.2 | 22 |
| 3 | Magic-sized CdSe nanoclusters for efficient visible-light-driven hydrogen evolution. Nano Research, 2022, 15, 3106-3113. | 5.8 | 16 |
| 4 | Plasmon-Boosted Fe, Co Dual Single-Atom Catalysts for Ultrasensitive Luminol-Dissolved O ₂ Electrochemiluminescence Detection of Prostate-Specific Antigen. Analytical Chemistry, 2022, 94, 9758-9765. | 3.2 | 35 |
| 5 | Synthesis of Lead-Free Cs ₂ AgBiX ₆ (X = Cl, Br, I) Double Perovskite Nanoplatelets and Their Application in CO ₂ Photocatalytic Reduction. Nano Letters, 2021, 21, 1620-1627. | 4.5 | 140 |
| 6 | Two-Dimensional-Plasmon-Boosted Iron Single-Atom Electrochemiluminescence for the Ultrasensitive Detection of Dopamine, Hemin, and Mercury. Analytical Chemistry, 2021, 93, 9949-9957. | 3.2 | 42 |
| 7 | Plasmon-Boosted Cu-Doped TiO ₂ Oxygen Vacancy-Rich Luminol Electrochemiluminescence for Highly Sensitive Detection of Alkaline Phosphatase. Analytical Chemistry, 2021, 93, 15183-15191. | 3.2 | 25 |
| 8 | Colloidal Semiconductor Quantum Dot–Based Multicomponent Artificial System for Hydrogen Photogeneration. , 2020, , 347-377. | | 0 |
| 9 | Stereoselective Câ^'C Oxidative Coupling Reactions Photocatalyzed by Zwitterionic Ligand Capped CsPbBr ₃ Perovskite Quantum Dots. Angewandte Chemie, 2020, 132, 22752-22758. | 1.6 | 16 |
| 10 | Stereoselective Câ^'C Oxidative Coupling Reactions Photocatalyzed by Zwitterionic Ligand Capped CsPbBr ₃ Perovskite Quantum Dots. Angewandte Chemie - International Edition, 2020, 59, 22563-22569. | 7.2 | 73 |
| 11 | Oriented bacteriorhodopsin/polyaniline hybrid bio-nanofilms as photo-assisted electrodes for high performance supercapacitors. Journal of Materials Chemistry A, 2020, 8, 8268-8272. | 5.2 | 16 |
| 12 | Effects of Illumination and Ferroelectric Field on Nanoscale Al:ZnO Films: Implications for Nonvolatile Multistage Storage and Photosensor Devices. ACS Applied Nano Materials, 2020, 3, 6054-6060. | 2.4 | 1 |
| 13 | Enhancing Photothermal Effect and Stability of Plasmonic Pd/Agâ€Nanosheet by Nanoassembly for Efficient Lightâ€Driven Catalytic Organic Hydrogenation. ChemistrySelect, 2019, 4, 13173-13181. | 0.7 | 4 |
| 14 | Pd/Ag nanosheet as a plasmonic sensing platform for sensitive assessment of hydrogen evolution reaction in colloid solutions. Nano Research, 2018, 11, 2093-2103. | 5.8 | 13 |
| 15 | Plasmonics Yields Efficient Electron Transport via Assembly of Shell-Insulated Au Nanoparticles. IScience, 2018, 8, 213-221. | 1.9 | 27 |
| 16 | Controlled Decoration of Divalent Nickel onto CdS/CdSe Core/Shell Quantum Dots to Boost Visibleâ€Lightâ€Induced Hydrogen Generation in Water. ChemPlusChem, 2018, 83, 1088-1096. | 1.3 | 3 |
| 17 | Boosting Electrocatalytic Oxygen Evolution Performance of Ultrathin Co/Ni-MOF Nanosheets via Plasmon-Induced Hot Carriers. ACS Applied Materials & Interfaces, 2018, 10, 37095-37102. | 4.0 | 67 |
| 18 | Combining the post synthesis ligand-assisted technique and SILAR method to assemble the quantum dots onto the oxide semiconductor photoelectrodes and its applications for solar cells. Journal of Alloys and Compounds, 2018, 765, 324-334. | 2.8 | 6 |

PING WANG

| # | Article | IF | CITATIONS |
|----|---|------|-----------|
| 19 | Plasmon-driven water splitting enhancement on plasmonic metal–insulator–semiconductor hetero-nanostructures: unraveling the crucial role of interfacial engineering. Nanoscale, 2018, 10, 14290-14297. | 2.8 | 25 |
| 20 | Photoelectrical properties of CdS/CdSe core/shell QDs modified anatase TiO ₂ nanowires and their application for solar cells. Physical Chemistry Chemical Physics, 2017, 19, 15724-15733. | 1.3 | 24 |
| 21 | Shell Thickness Engineering Significantly Boosts the Photocatalytic H ₂ Evolution Efficiency of CdS/CdSe Core/Shell Quantum Dots. ACS Applied Materials & Interfaces, 2017, 9, 35712-35720. | 4.0 | 48 |
| 22 | Long-Range Plasmon Field and Plasmoelectric Effect on Catalysis Revealed by Shell-Thickness-Tunable Pinhole-Free Au@SiO ₂ Core–Shell Nanoparticles: A Case Study of <i>p</i> -Nitrophenol Reduction. ACS Catalysis, 2017, 7, 5391-5398. | 5.5 | 73 |
| 23 | Enhanced photovoltaic performance of dye-sensitized solar cells using a new photoelectrode material: upconversion YbF ₃ -Ho/TiO ₂ nanoheterostructures. Nanoscale, 2016, 8, 4173-4180. | 2.8 | 56 |
| 24 | Bacteriorhodopsin/Ag Nanoparticle-Based Hybrid Nano-Bio Electrocatalyst for Efficient and Robust H ₂ Evolution from Water. Journal of the American Chemical Society, 2015, 137, 2840-2843. | 6.6 | 59 |
| 25 | The important role of surface ligand on CdSe/CdS core/shell nanocrystals in affecting the efficiency of H ₂ photogeneration from water. Nanoscale, 2015, 7, 5767-5775. | 2.8 | 75 |
| 26 | Graphene Oxide-Supported Ag Nanoplates as LSPR Tunable and Reproducible Substrates for SERS Applications with Optimized Sensitivity. ACS Applied Materials & Interfaces, 2015, 7, 18038-18045. | 4.0 | 65 |
| 27 | The facile surface chemical modification of a single glass nanopore and its use in the nonenzymatic detection of uric acid. Chemical Communications, 2015, 51, 1914-1917. | 2.2 | 25 |
| 28 | Lightâ€Ðriven, Membraneless, Hydrogen Peroxide Based Fuel Cells. Advanced Energy Materials, 2015, 5, 1400424. | 10.2 | 40 |
| 29 | Significantly Enhancing Supercapacitive Performance of Nitrogen-doped Graphene Nanosheet Electrodes by Phosphoric Acid Activation. ACS Applied Materials & Interfaces, 2014, 6, 1563-1568. | 4.0 | 57 |
| 30 | High-Efficiency Plasmon-Enhanced and Graphene-Supported Semiconductor/Metal Core–Satellite Hetero-Nanocrystal Photocatalysts for Visible-Light Dye Photodegradation and H ₂ Production from Water. ACS Applied Materials & Interfaces, 2014, 6, 19905-19913. | 4.0 | 33 |
| 31 | Efficient visible light-driven H ₂ production in water by CdS/CdSe core/shell nanocrystals and an ordinary nickel–sulfur complex. Nanoscale, 2014, 6, 13470-13475. | 2.8 | 41 |
| 32 | Facile synthesis of a free-standing Ag@AgCl film for a high performance photocatalyst and photodetector. Chemical Communications, 2013, 49, 4953. | 2.2 | 50 |
| 33 | Flexible graphene–polyaniline composite paper for high-performance supercapacitor. Energy and Environmental Science, 2013, 6, 1185. | 15.6 | 970 |
| 34 | Effect of BiVO ₄ Crystalline Phases on the Photoinduced Carriers Behavior and Photocatalytic Activity. Journal of Physical Chemistry C, 2012, 116, 2425-2430. | 1.5 | 245 |
| 35 | Shape Transformation and Visible Region Plasmonic Modulation of Silver Nanoplates by Graphene Oxide. Small, 2012, 8, 3438-3442. | 5.2 | 11 |
| 36 | The dependence of photocatalytic activity and photoinduced self-stability of photosensitive AgI nanoparticles. Dalton Transactions, 2012, 41, 10405. | 1.6 | 87 |

PING WANG

| # | Article | IF | CITATIONS |
|----|---|-----|-----------|
| 37 | Progress in graphene-based photoactive nanocomposites as a promising class of photocatalyst. Nanoscale, 2012, 4, 5814. | 2.8 | 143 |
| 38 | Controlled synthesis of porous Ag/Au bimetallic hollow nanoshells with tunable plasmonic and catalytic properties. Nano Research, 2012, 5, 135-144. | 5.8 | 108 |
| 39 | Superparamagnetic Plasmonic Nanohybrids: Shape-Controlled Synthesis, TEM-Induced Structure Evolution, and Efficient Sunlight-Driven Inactivation of Bacteria. ACS Nano, 2011, 5, 8562-8570. | 7.3 | 68 |
| 40 | Synthesis of reduced graphene oxide-anatase TiO2 nanocomposite and its improved photo-induced charge transfer properties. Nanoscale, 2011, 3, 1640. | 2.8 | 170 |
| 41 | Facile solvothermal synthesis of cube-like Ag@AgCl: a highly efficient visible light photocatalyst. Nanoscale, 2011, 3, 2931. | 2.8 | 191 |
| 42 | Dual-functional Au–Fe3O4 dumbbell nanoparticles for sensitive and selective turn-on fluorescent detection of cyanide based on the inner filter effect. Chemical Communications, 2011, 47, 8268. | 2.2 | 76 |
| 43 | Facile synthesis of two-dimensional graphene/SnO2/Pt ternary hybrid nanomaterials and their catalytic properties. Nanoscale, 2011, 3, 4376. | 2.8 | 73 |
| 44 | Aqueous-phase synthesis of Ag-TiO2-reduced graphene oxide and Pt-TiO2-reduced graphene oxide hybrid nanostructures and their catalytic properties. Nano Research, 2011, 4, 1153-1162. | 5.8 | 63 |
| 45 | Hydrothermal synthesis and photoelectric properties of BiVO4 with different morphologies: An efficient visible-light photocatalyst. Applied Surface Science, 2011, 257, 7758-7762. | 3.1 | 87 |
| 46 | Synthesis of highly efficient C-doped TiO2 photocatalyst and its photo-generated charge-transfer properties. Journal of Colloid and Interface Science, 2011, 354, 175-180. | 5.0 | 123 |
| 47 | Size- and photoelectric characteristics-dependent formaldehyde sensitivity of ZnO irradiated with UV light. Sensors and Actuators B: Chemical, 2010, 148, 66-73. | 4.0 | 55 |
| 48 | One-step, solvothermal synthesis of graphene-CdS and graphene-ZnS quantum dot nanocomposites and their interesting photovoltaic properties. Nano Research, 2010, 3, 794-799. | 5.8 | 177 |
| 49 | Facile synthesis of TiO2(B) crystallites/nanopores structure: A highly efficient photocatalyst. Journal of Colloid and Interface Science, 2010, 350, 417-420. | 5.0 | 7 |
| 50 | One-pot, water-phase approach to high-quality graphene/TiO2 composite nanosheets. Chemical Communications, 2010, 46, 7148. | 2.2 | 183 |
| 51 | Synthesis and Plasmonâ€Induced Chargeâ€Transfer Properties of Monodisperse Goldâ€Đoped Titania Microspheres. Chemistry - A European Journal, 2009, 15, 4366-4372. | 1.7 | 100 |
| 52 | Synthesis and Studies of the Visibleâ€Light Photocatalytic Properties of Nearâ€Monodisperse Biâ€Doped TiO ₂ Nanospheres. Chemistry - A European Journal, 2009, 15, 12521-12527. | 1.7 | 112 |
| 53 | Ultraviolet-assisted gas sensing: A potential formaldehyde detection approach at room temperature based on zinc oxide nanorods. Sensors and Actuators B: Chemical, 2009, 136, 80-85. | 4.0 | 136 |
| 54 | The enhancement of oxygen sensitivity of ZnO macropore film by functionalizing with azo pigment. Photochemical and Photobiological Sciences, 2009, 8, 875. | 1.6 | 6 |

PING WANG

| # | Article | IF | CITATIONS |
|----|---|-----|-----------|
| 55 | Light induced enhancing gas sensitivity of copper-doped zinc oxide at room temperature. Sensors and Actuators B: Chemical, 2008, 131, 660-664. | 4.0 | 70 |
| 56 | Anomalous photoconductivity of cobalt-doped zinc oxide nanobelts in air. Chemical Physics Letters, 2008, 456, 231-235. | 1.2 | 43 |
| 57 | Preparation of monodisperse Ag/Anatase TiO2 core–shell nanoparticles. Materials Chemistry and Physics, 2008, 109, 181-183. | 2.0 | 18 |
| 58 | Water-Assisted Synthesis of Anatase TiO ₂ Nanocrystals:  Mechanism and Sensing Properties to Oxygen at Room Temperature. Journal of Physical Chemistry C, 2008, 112, 6648-6652. | 1.5 | 41 |
| 59 | Photovoltaic properties of a ZnO nanorod array affected by ethanol and liquid-crystalline porphyrin. Nanotechnology, 2008, 19, 245706. | 1.3 | 41 |
| 60 | Size- and Orientation-Dependent Photovoltaic Properties of ZnO Nanorods. Journal of Physical Chemistry C, 2007, 111, 17136-17145. | 1.5 | 109 |
| 61 | A facile solution-phase synthesis of high quality water-soluble anatase TiO2 nanocrystals. Journal of Colloid and Interface Science, 2007, 314, 337-340. | 5.0 | 39 |
| 62 | Microporous Metal–Organic Framework Constructed from Heptanuclear Zinc Carboxylate Secondary Building Units. Chemistry - A European Journal, 2006, 12, 3754-3758. | 1.7 | 159 |
| 63 | A New Highly Selective H2Sensor Based on TiO2/PtOâ^'Pt Dual-Layer Films. Chemistry of Materials, 2002, 14, 3953-3957. | 3.2 | 96 |
| 64 | Plasmonics Yields Surprisingly Efficient Electron Transport Via Assembly of Shell-Insulated Au Nanoparticles. SSRN Electronic Journal, 0, , . | 0.4 | 0 |